Research Article

Melatonin synthesized by activated microglia orchestrates the progression of microglia from a pro-inflammatory to a recovery/repair phenotype

Ewerton S. Souza[1], Adriessa A. Santos[1], Edson E.D. Ribeiro-Paz[1], Marlina Córdoba-Moreno[1], Isabela L Trevisan[1], Waldir Caldeira[2], Sandra M. MuxelM[1], Kassiano D.S. Sousa.[1], Regina P. Markus.[1]*

[1] Department of Physiology, Bioscience Institute., University of São Paulo, BR
[2] Department of Genetics and Evolutionary Biology, Bioscience Inst., USP, BR
* Correspondence: rpmarkus@usp.br; Tel: +55(11)981991818

Running title: Melatonin and cerebellar microglia phenotypes

Received: January 6, 2022; Accepted March 28, 2022

ABSTRACT

Microglia, the sentinels of the central nervous system, are responsible for the surveillance and the innate defense against pathogen or danger/damage-associated molecular patterns. The response is fine-tuned to restrain pro-inflammatory responses, preserving neighboring cells. At the injured area, microglia temporarily shift to a pro-inflammatory phenotype (M1), followed by anti-inflammatory (M2) phenotypes. The duration and magnitude of the pro-inflammatory phase are finely regulated to avoid unnecessary loss of brain tissue. The present study shows that melatonin synthesized by microglia plays a key role in the transformation of M1 to M2 phenotypes. In a mixed rat cerebellar glia culture, the percentage of activated microglia did not vary significantly with the treatments, while the role of melatonin synthesized by microglia in promoting the end of the pro-inflammatory phase, and the initiation of the regulatory/phagocytic phases was inferred by using pharmacological tools. Total microglia were identified by the expression of CD11b/c, whereas positive to IBA-1 microglia were considered activated, independent of the phenotype. M1 and M2 phenotypes were distinguished with the biomarkers NOS-2 and ARG-1, as these enzymes act on the same substrate (L-arginine), producing pro-inflammatory (NO) or anti-inflammatory (polyamines and proline) end products, respectively. Luzindole, a blocker of melatonin receptors, impaired the conversion of M1 to M2 phenotypes and zymosan phagocytosis. Thus, melatonin content synthesized by cerebellar microglia determines the extension of the pro-inflammatory phase of defense response.

Key words: extra-pineal melatonin, cerebellum, microglia activation, phagocytosis, recovery microglia, acute inflammatory response

---

1. INTRODUCTION

Acute inflammation, also known as innate immune response, is a stereotyped reaction to injury. Under the baseline conditions, multiple motile processes of stellate microglia (M0) actively

monitor the local environment. Upon activation, microglia transform to an ameboid pro-inflammatory phenotype (M1), followed by to be the recovery/cleanup/repair phenotype (M2), and then return to the basal M0 phenotype (1, 2). Despite specificities linked to injury type and microglia localization, the immediate defense response's success relies on timing M1 to M2 phenotype shift. The pro-inflammatory phase's duration and magnitude should be fine-tuned by a programmed delay between the expression of pro-inflammatory and anti-inflammatory mediators.

The transcription nuclear factor kappa B (NF-κB), a dimer sequestered in the cytoplasm by its interaction with inhibitory κB proteins, mediates M0 to M1 shift (3). Canonical and non-canonical pathways of NF-κB activation are responsible for the variety of outputs. The defense response ends by restoring the extracellular environment, or progresses to develop neuro-pathologies (4-6).

At the beginning of an acute inflammatory response, the dimer p50/RelA is translocated to the nucleus interacts with kappa B elements in the promoter of genes that code pro-inflammatory cytokines and enzymes. It also leads to the expression of another NF-κB subunit, cREL, which forms dimers that migrate to the nucleus (7). Dimers containing cREL induce the transcription of the serotonin-N-acetyltransferase (SNAT, formally AANAT) coding gene (8). SNAT is the key enzyme in melatonin synthesis, as it converts serotonin into N-acetylserotonin, which is then, methylated to form melatonin. NF-κB-dependent induction of melatonin synthesis was already shown in rodents, and humans activated macrophages and microglia *in vitro*, *in silica*, and *in situ* (9-11). Melatonin was shown to inhibit excessive microglial activation (12).

Besides reducing pro-inflammatory mediators' expression, melatonin also increases the expression of M2 phenotype biomarkers, such as interleukine-10 (IL-10) and arginase-1 (Arg-1) (13). Therefore, a candidate for orchestrating M1 to M2 passage. In addition, the time elapsed between activation of the NF-kB pathway by pathogen- or damage-related molecular patterns (PAMPs, DAMPs) and the expression of SNAT and melatonin synthesis could determine M1 to M2 phenotype shift (Figure 1).

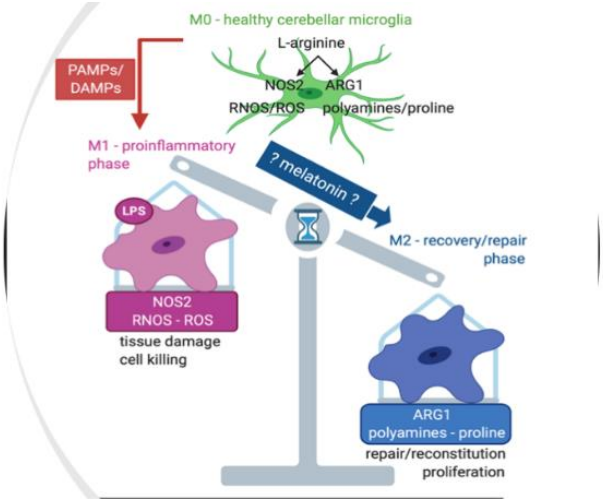

Fig. 1. Working hypothesis – Surveillance cerebellar microglia metabolizes L-arginine via NOS-2 and ARG-1 pathways.

ARG-1 pathway, responsible for surveillance and proliferation, is shared by many cells, while NOS-2 basal activity is characteristic of partially depolarized cerebellar microglia found in healthy conditions (14). Lipopolysaccharide (LPS) induces a stereotyped response initiated by microglia activated at the M1 phenotype. Invaders and neighboring cells are killed and the

extracellular matrix damaged. This phenotype needs to evolve to enable matrix repair, replacement of injured cells, and phagocytosis of cellular debris and foreign elements (M2 phenotypes). We hypothesize that cerebellar microglia melatonin synthesis starts at the end of the pro-inflammatory phase, being a key element in the transition between M1 and M2.

Here we evaluated whether melatonin orchestrates the transition from M1 to M2 phenotypes by determining the expression of nitric oxide synthase-2 (NOS-2) and ARG-1 in cultured cerebellar microglia challenged with LPS in the presence or absence of melatonin receptor blockage. Accordingly, high-affinity receptors detect microglia synthesized melatonin and trigger phenotype progression.

2. MATERIAL AND METHODS

2.1. Animals.

Postnatal day (P1 to P5) Wistar rat pups were obtained from the Central Animal Facility of the Institute of Biomedical Sciences of the University of São Paulo, Brazil. All animal procedures were conducted following the regulatory standards of the National Council for Control in Animal Experimentation (CONCEA) and were approved by the Animal Use Ethics Commission (CEUA) of the Institute of Biosciences, University of São Paulo (protocol 159/2012 and 198/2014).

2.2. Material, reagents, drugs and antibodies.

All chemicals and biological material are listed in the supplemental material Table 1.

2.3. Cell culture.

Primary mixed glial cell cultures were modified from the described methods (15, 16). The heads of decapitated pups were placed in 70% ethanol, the cerebellum isolated, and immersed in PBS (1 mL, PBS; 8g NaCl, 0.2 g KCl, 1.44 g Na2HPO4, 0.24 g KH2PO4) plus 5% of bovine serum albumin (BSA). The meninges were removed, the tissue pricked, and the cells dispersed with a neural tissue dissociation kit. The homogenate was filtered in a 100 µm cell strainer, centrifuged (400g, 5 min, room temperature, RT), and the cells were resuspended in 2 mL of Dulbecco's modified Eagle's medium (DEMEM) supplemented with 100 IU/mL penicillin and 100µg/mL streptomycin (pen/strep) and 10% fetal bovine serum (FBS). Cells were seeded in 24-well plates with $2x10^6$ cells/well for flowsight cytometry analysis or in 8-well chamber slides with $5x10^5$ cells/well to obtain images in confocal microscopy. The cultures were maintained in 200µL DMEM at 37°C, 5% CO2, for seven days with a medium change on day 5. One hour before treatments, the medium was replaced by DMEM without FBS. All the procedure was done in a sterile environment. Viability and cell number were estimated by Trypan blue exclusion.

For phagocytosis assays, enriched microglia cultures were prepared from the mixed cell cultures maintained for 15 days in 75 cm^2 cell culture flasks containing DMEM plus 10% FBS and pen/strep. The cells were incubated in a DMEM without FBS one hour before the treatments. Microglia were mechanically isolated by knocking flasks twice or three times on the bench and seeded (10^5 cells/ 200 µL DMEM) in 8-well chamber slides for seven days (37°C, 5% CO2). Medium with FBS was replaced every 48 hours.

2.4. Flowsight cytometry.

For seven days, mixed cerebellar glial cells were maintained in 24-well plates ($2x10^6$ cells/well). The medium was discarded after experimental procedures, 200µL of cold PBS was added to the plate, and cells were scraped and placed in 1.5 mL microtubes. The content was centrifuged (400g, 5 min, RT), and the supernatant was discarded. Cells were fixed in 150µL PFA (5% in PBS, 15 min), and after centrifugation (400g, 5 min, RT), the pellet was resuspended in 150µL of Triton-X (0.1% in PBS, 15 min) and then in PBS containing BSA (5%). In sequence, cells were incubated 1 hour at room temperature with anti-CD11b/c PECy7 conjugated (1:500) antibody as a microglial biomarker, plus anti-IBA-1 (1:500, biomarker of activated microglia M1 to M2), anti-NOS-2 (1:500, biomarker M1 phenotype) or anti-ARG-1 (1:500, M2 phenotype) for identifying total activated, pro-inflammatory or recovery/repair subtypes. Cells were washed three times with PBS and incubated for 1 hour with the appropriate secondary antibody, donkey anti-rabbit PercP-Cy5.5 (1:1000), or goat anti-mouse PECy7 (1:1000). After washing the cells with PBS, 100 µL of BSA was added (5% in PBS). Cell nuclei were marked with propidium iodide (PI, 1:10000), added 5 min before sample acquisition. The samples were acquired using AMNIS® FlowSight® (Luminex, Austin, TX, USA) flow cytometry, and data were analyzed with IDEAS® software® (Luminex, Austin, TX, USA).

2.5. Phenotype characterization.

For cell visualization, mixed glial cells were cultured in 8-well chamber slides ($5x10^5$ cells/well) for seven days and cells were fixed with paraformaldehyde (PFA - 5% in PBS, 15 min, RT), permeabilized with Triton-X (0.1% in PBS, 10 min, RT), and blocked with BSA (2% in PBS, 1 hour, RT). Microglia and astrocytes were identified with the antibodies anti-CD11b FITC (1:1000) and anti-GFAP AF488 (1:2000), incubated for 1 h at RT followed by three washes with PBS. The slides were then fixed with Mounting Medium with DAPI, and images were captured using the Zeiss LSM 880 (Axio Observer) confocal microscope equipped with a 20x EC Plan-Neofluar objective. For excitation of FITC and Alexa Fluor 488 fluorophores (green), the Argon 488 nm laser was used with an emission range of 505-550 nm. DAPI (blue) was excited using a Diode 405 nm laser with a 410-490 nm emission range. Microglial phenotypes and percentages in mixed glial cell cultures were determined by flowsight cytometry analysis. Microglia were identified as nucleated (PI+, propidium iodide)/ CD11b/c+ cells population and represent 3 – 10% of total single cells acquired (Supplemental figure 1). Microglia activation and phenotypes were addressed by evaluating the protein expression of IBA-1 (all activated), NOS-2 (M1), and ARG-1 (M2) after treatment with lipopolysaccharide (LPS,100ng/mL) or LPS plus minocycline (300µM). Control groups were incubated with MINO or vehicle (medium). After experimental procedures, the samples were prepared for flowsight cytometry analysis. The protein expression of the microglia activation biomarkers (IBA-1, NOS-2, and ARG-1) was determined based on the mean fluorescence intensity emitted in PI+/CD11b/c+ cells.

2.6. Phagocytosis assay.

The phagocytosis of zymosan by microglia was determined by flowsight cytometry in mixed glial cell cultures. The cultures were maintained in 24-well plates for seven days. Cells were incubated with zymosan conjugated with Alexa Fluor 488 (105 particles/well, 75 min) with or

without MINO (300µM) incubated for one hour before zymosan added. Phagocytic activity was determined by the mean fluorescence intensity of zymosan particles conjugated to AF488 in the PI+/CD11b/c+ cell population.

The effects of melatonin and luzindole on the phagocytic capacity were determined in microglia enriched cultures incubated with zymosan conjugated with AF594 in 8-well chamber slides (105 particles/well) for 75 min. Cultures were incubated with melatonin (0 – 100 nM) or luzindole (0 – 1000 nM) for 30 min before zymosan addition. Cells were fixed with acetone and methanol (1:1, 15 min, RT), and the slides were analyzed using Zeiss LSM 510 confocal microscope using a 63x/1.2 objective lens with water immersion. Fluorescent zymosan was excited with HeNe 543 nm laser, and the fluorescence emission was measured at 560-615 nm. Photographs were taken randomly from four fields in each well with a resolution of 1024 x 1024 pixels with fixed parameters (pinhole, scanning speed, and laser power). Cells that phagocytized one or more zymosan particles were adopted as counting criteria.

2.7. Characterizing the relevance of microglia melatonin for the transition from M1 to M2 phenotype.

Cells were cultured in 24-wells plates and maintained for seven days before treatments. The cells were incubated with luzindole (100 nM) for one h, and LPS (100 ng/ mL) was then added and maintained for 12h. Luzindole is a non-selective MT1 and MT2 melatonin receptors (17). After the experimental procedures, the samples were prepared for flowsight cytometry analysis (as described in the flowsight cytometry section). Samples were acquired using Amnis® Flowsight® flow cytometry (Luminex, Austin, TX, USA), and data were analyzed with IDEAS® software.

2.8 Statistical analysis.

All the numbers shown refer to individual cultures means and not isolated replicates. Statistical analysis was performed with GraphPad Prism 9.0 software. Independent variables are presented as box plot whiskers (10%-90%), and dependent variables (time-dependent) are presented as the mean ± SEM (standard error of the mean). These data were compared by fitting the data to non-linear regressions, and the goodness of fitting was tested by ANOVA. Differences between independent variables were evaluated by Kolmogorov-Smirnov or ANOVA for nonparametric values, followed by the Mann-Whitney or Kruskal-Wallis/Dunn's tests.

3. RESULTS

3.1. Microglia phenotypes after 12h-LPS incubation.

First, we established an experimental protocol in which the percentage of microglia (CD11b/c+) in culture was not altered by incubation with melatonin receptor antagonists, inhibition of microglial activation, and induction of an acute inflammatory response. Confocal images confirm the presence of astrocytes (GFAP+) and microglia (CD11b/c+) in naïve cultures. Microglia present phyllopod and are much smaller than astrocytes (Figure 2A). 3-10% of the cells sorted in a flowsight cytometer were CD11b/c+ positive (microglia), and this percentage was maintained after being incubated for 12 hours with luzindole (100 nM), minocycline (300µM), or LPS (100 ng/mL) (Figure 2B).

Figure 2C shows the time-course for microglia activation (ionized calcium-binding adapter molecule 1 (IBA-1) expression) and its blockage by minocycline, an inhibitor of microglia LPS-induced NF-κB activation (18, 19). We recorded the responses 6 and 12 hours after incubation, therefore after the pro-inflammatory peak. Notably, the peak of the inflammatory response (high NOS-2) occurs after 6 hours in LPS. The plateau was reached after 12 hours in LPS.

In sequence, we evaluated the effect of blocking LPS-induced activation with MINO (Figure 2D) in the expression of biomarkers for nonspecific (IBA-1), M1 (NOS-2), and M2 (ARG-1) phenotypes (figure 2D). Minocycline blocked LPS-induced increased IBA-1, NOS-2, and ARG-1 and had no effect on cultures incubated with the vehicle. Thus, MINO blocked the mounting of the acute inflammatory response. The enzymes that metabolize L-arginine (NOS-2 and ARG-1) already expressed in M0 (20, 21) were differentially affected by LPS (12h). ARG-1 but not NOS-2 was significantly expressed over the vehicle, confirming that the cells had already shifted to M2 phenotype.

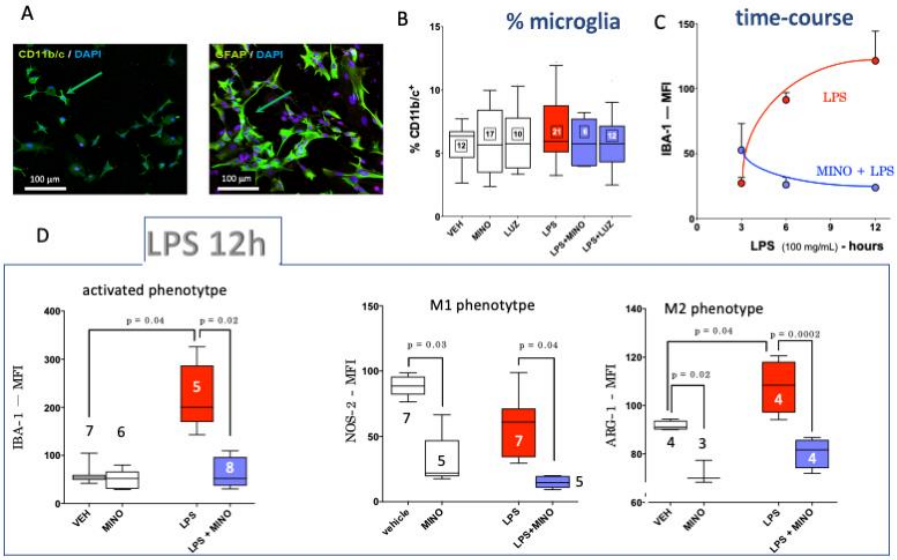

Fig.2. Characterization of the experimental model in primary mixed cerebellar glial cell culture.

(A): confocal micrograph highlighting the presence of microglia (CD11b/c+) and astroglia (GFAP+). (B) The percentage of microglia was maintained independently of the treatments. (C) Time-course (3 - 12 h) of LPS (100 ng/mL)-induced microglial activation (IBA-1 expression). IBA-1 marks any activated phenotype. It is noteworthy that the pro-inflammatory phase (NOS-2 peak) occurred before the third hour of incubation. (D) Twelve hours after LPS, inhibiting microglial activation by minocycline blocks NOS-2 and ARG-1 expression induction. Boxes show data medians, and whiskers represent percentiles 10-90%. Data were tested with the Kruskal-Wallis Multiple Comparison test. The number of independent cultures and the probability of rejecting a null hypothesis are in the graph. VEH (vehicle), MINO (minocycline 300 µM), LPS (lipopolysaccharide, 100 ng/mL).

3.2 Autocrine melatonin increases microglia phagocytic efficiency.

Zymosan recognition receptors (TLR2/TLR6) trigger melatonin synthesis (11, 22), and macrophage synthesized melatonin increases the expression of dectin-1, a membrane protein that

mediates zymosan phagocytosis 11. Here we observed that zymosan (100.000 particles, 75 min) microglia phagocytosis was blocked by inhibiting microglia activation with minocycline (Figure 3A) and by blocking melatonin receptors with luzindole (Figure 3B). Otherwise, incubating the cultures with melatonin induces zymosan phagocytosis (Figure 3B). Reinforcing the conclusion that culture-synthesized melatonin acts via melatonin receptors, the pKi value for luzindole (8.15 ± 0.20) was in the range accepted for blocking MT2 melatonin receptor (17).

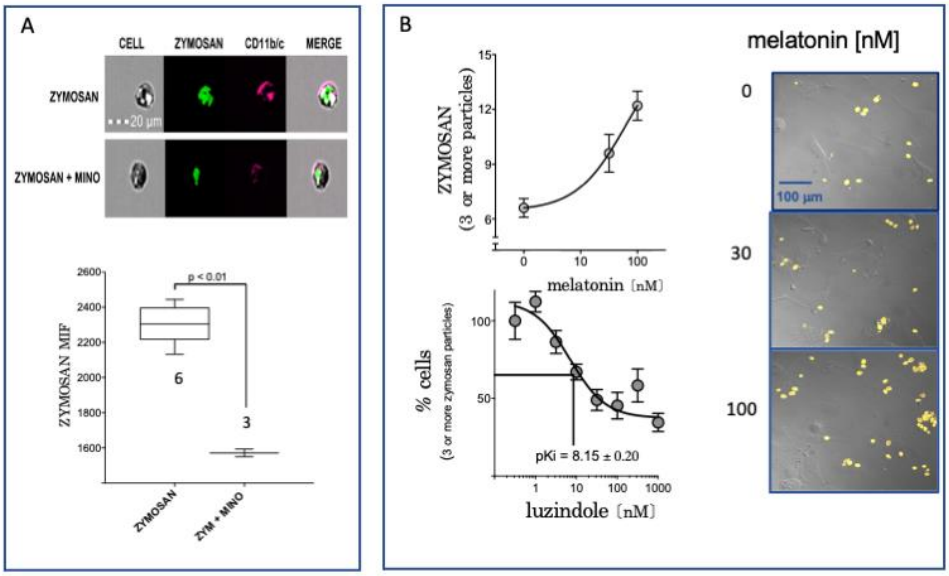

Fig. 3. Effect of autocrine melatonin on the phagocytosis of zymosan particles.

(A) Phagocytosis of zymosan (105 particles/well, one h) by activated microglia (CD11 b/c+) is blocked by minocycline (MINO 300 µM) incubated one hour before zymosan. Data are shown as the median in box and whiskers (percentiles 10-90%), and the difference between means was determined by Student's "t" test. The number of independent cultures is shown in the graph.
(B) Phagocytosis of fluorescent zymosan particles (105 particles/well, 75 min) by enriched microglia cultures visualized by confocal microscopy. Incubation of exogenous melatonin potentiated, while the blockage of melatonin high-affinity G-protein coupled receptors with luzindole inhibited zymosan uptake. Thus, microglia synthesized melatonin potentiates microglial phagocytosis. Data are shown as mean +/- s.e.m. of 5 independent cultures in the upper graph and 5-12 in the lower one. Data were fitted to a sigmoidal curve by the least square method.

3.3. Effects of microglia-synthesized melatonin on phenotype transition.

To determine if melatonin synthesized at the transition between M1 and M2 is essential for phenotype shift, we evaluated the expression of NOS-2 and ARG-1. The blockage of melatonin receptors with luzindole increased NOS-2 and reduced ARG-1 expression in LPS-activated microglia (Figure 4). Notably, the expression of IBA-1 that occurs in both M1 and M2 cells is increased by LPS and only marginally inhibited by luzindole (tested significantly only when both means were compared with the Kolmogorov-Smirnov test). Therefore, despite not altering the quantity of activated microglia, luzindole impaired the shift from the M1 to M2 phenotype, indicating that melatonin synthesized at the transition between M1 and M2 is essential for phenotype progression.

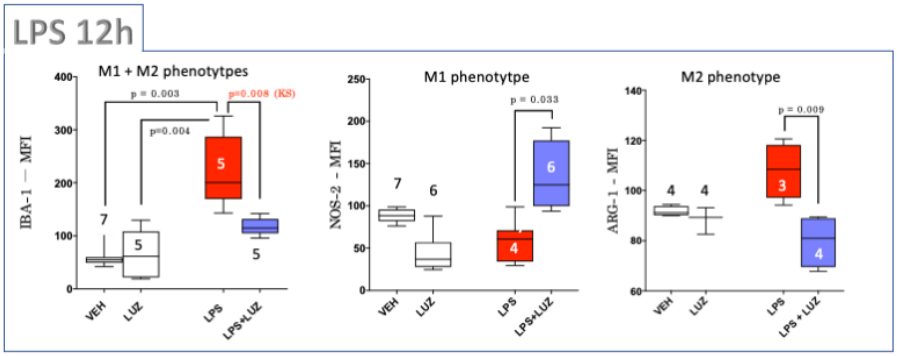

Fig. 4. Melatonin and the transition between M1 to M2 phenotype.

Mix cerebellar glial cell cultures were incubated with luzindole (LUZ, 100 nM) for one hour before a stimulus of 12 hours with LPS (100 ng/ mL). Microglia were identified with the biomarker CD11b/c+. LPS leads to a significant increase in activated microglia (IBA-1 biomarker). Blocking melatonin receptors with luzindole increases M1 (NOS-2 biomarker) and reduces M2 phenotype (ARG-1 biomarker), indicating that microglia did not progress from a proinflammatory to a recovery/ repair phenotype. Data were plotted as boxes and whiskers (10 – 90%). The probability of rejecting the null hypothesis was determined by Kruskal-Walls followed by Dunn's multiple comparisons test. The pair LPS versus LPS + LUZ was not significantly different when the non-parametric ANOVA was applied, and the Kolmogorov-Smirnov test obtained the probability shown in the figure. The number of independent cultures is shown in the figure.

4. DISCUSSION

Acute inflammatory defense responses triggered by noxious stimuli must be temporally restricted to avoid unnecessary damages (1, 23). As a pharmacological tool, melatonin inhibits hippocampus expression of pro-inflammatory cytokines in *Klebsiella pneumonia* inoculated mice (24*)* and the levels of TNF and NO in cortical microglia of LPS injected rats (25), polarizing microglia to resolution phenotypes (24, 26, 27, 28, 29). Accordingly, to the increased phagocytic capacity of these cells, melatonin incubation increases colostral macrophage expression of dectin-1, a key molecule in zymosan phagocytosis (11).

Melatonin synthesized by challenged monocytes, macrophages, and microglia plays a role in solving inflammatory responses by inducing phagocytosis of microorganisms and DAMP and reducing the death of neighbor cells. The synthesis of melatonin by human colostrum monocytes (30), RAW 264-7 cell line (22), and rat alveolar macrophages (9) potentiates phagocytosis. The microglia synthesized melatonin reduces LPS-induced neurotoxicity (31), signaled by NF-kB (21).

Here we investigated whether microglia synthesized melatonin could be responsible for temporizing inflammatory response, converting microglia from a pro-inflammatory to a resolution phenotype. Our strategy was distinguishing microglia phenotypes in mixed astrocyte microglia cerebellar culture, which maintain the same number of cells when challenged with LPS, avoiding misinterpretations induced by selective loss of one phenotype. During 12 hours of incubation with LPS, the membrane expression of IBA-1, which interacts with F-actin and is essential for membrane ruffling and phagocytosis, followed a hyperbolic curve (32). Inhibiting IBA-1 expression with minocycline confirmed that LPS-induced activation of the NF-kB pathway was essential for this biomarker that did not distinguish M1 from M2 microglia (33, 34).

Loops of inducing/repressing gene expression and protein synthesis are the basis for reaching a successful defense response (20, 35). The progression of an inflammatory response involves the shift of L-arginine metabolism due to sequential expression and activation of two enzymes. Initially, the increase in NOS-2 activity converts L-arginine into citrulline and NO, promoting oxidative stress (36). The transition between the pro-inflammatory and the resolution phase involves reducing NOS-2 and increased ARG-1 transcription and expression. ARG-1, the last enzyme in the urea cycle, converts L-arginine into urea and L-ornithine, contributing to the synthesis of polyamines and proline, essential for collagen formation and tissue repair (37). ARG-1 shows a positive relationship with neuroprotection (38). Choosing the two biomarkers for defining M1 and M2 phenotypes had the advantage of linking molecular expression to function. In our experimental conditions, microglia incubated for 12 hours with LPS were at the M2 phenotype, as the expression of ARG-1 was significantly higher than that of NOS-2 and developed an efficient phagocytic activity.

We confirm previous "*in vivo*" data showing that rat cerebellar microglia synthesize melatonin (31). Considering that blocking high-affinity melatonin receptors decreases/increases the expression of NOS-2/ ARG-1 and potentiates phagocytosis, we concluded that microglia synthesized melatonin progresses these defense cells from a pro-inflammatory to a recovery phenotype. Thus, the progression of an innate defense response begins with the activation of the NF-kB pathway, followed by nuclear translocation of the dimer p50/RelA, and the transcription of a package of genes that codify pro-inflammatory mediators, including NOS-2, as well as cRel protein-coding gene. As the dimer, p50/cRel triggers the transcription of SNAT, a key enzyme in melatonin synthesis, and melatonin inhibits/ triggers the synthesis of NOS-2/ ARG-1, the interval between the expression of cRel and the increased synthesis of melatonin determines the extension of the pro-inflammatory phase.

This is the first demonstration that microglia synthesized melatonin is a key molecule in determining the duration of innate defense responses, to the best of our knowledge. The potential mechanisms are illustrated in the Figure 5.

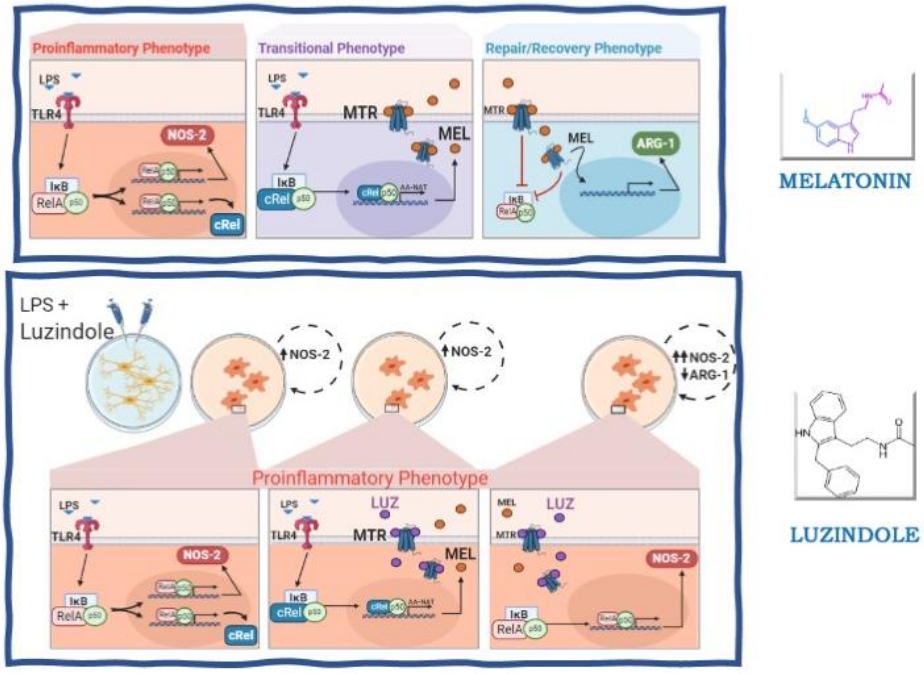

Fig. 5. Cerebellar microglia melatonin is a key element in shift pro-inflammatory (M1) to recovery/repair phenotypes (M2).

Upper panel: The hypothesis:

The effect of microglia synthesized melatonin is highlighted. Activation of TLR4 receptors by LPS leads to the nuclear translocation of the NF-κB dimer p50/RelA, which promotes not only the transcription of genes that code pro-inflammatory proteins but also the NF-κB subunit cREL. NOS-2, here used as a biomarker of the pro-inflammatory response, is among the first transcribed proteins. As the response progresses, the dimer p50/ cRel translocates to the nucleus, leading to the transcription of proteins involved in the recovery/repair phase. AA-NAT, a key enzyme in melatonin synthesis, is one of these proteins. In sequence, melatonin activates high-affinity G-protein coupled melatonin receptors leading to the synthesis of ARG-1, a biomarker of M2. The hypothesis was tested by blocking melatonin receptors with the non-selective competitive antagonist - luzindole.

Lower panel: Microglia melatonin - signalizes the time interval between M1 and M2.

Blocking melatonin receptors microglia are kept at M1 phenotype, and the inflammatory response is not solved. Here we show for the first time that microglia melatonin synthesis is essential for the progression of M1 to M2 phenotype. Therefore, if melatonin is not synthesized or their receptors are not expressed, no resolution of the inflammatory response will occur.

ACKNOWLEDGEMENTS

This study was supported by research grants # 2013/13691-1, São Paulo Research Foundation (FAPESP); #480097/2013-5, Scientific and Technological Development (CNPq) to RPM. KSS is a Scientific and Technological Development (CNPq) graduate fellow (processo # 140274/2018-9). RPM is a CNPq Senior Research. ESS, AS, EDRP, MCM, ILT and KSS were graduate fellows of the Coordination for the Improvement of the Higher Education Personnel (CAPES – finance code 001). The technical assistance of Debora Aparecida Moura (technical fellow of CNPq) is gratefully acknowledged. We thank Dr. Beatriz Pacheco Jordão for proofreading the English.

AUTHORSHIP

RPM: Conceived the study. ESS and RPM: Designed the study. RPM provided essential resources for the study. ESS, AS, EDRP, MCM, ILT, WC and SMM performed experiments and processed the data. ESS, KSS and RPM performed the formal analysis of the data. ESS, AS, KSS and RPM interpreted the data. KSS and RPM prepared the figures. ESS, ILT, KSS and RPM wrote the manuscript. All authors edited, revised and approved the final version of the manuscript.

CONFLICT OF INTEREST

The authors declare no competing interests.

DATA AVAILABILITY

The data that support the findings of this study are available from the corresponding author upon reasonable request.

REFERENCES

1. Hanisch UK (2013). Functional diversity of microglia - How heterogeneous are they to begin with? *Front. Cell Neurosci*. **7**: 1–18.
2. Stence N, Waite M, Dailey ME (2001). Dynamics of microglial activation: A confocal time-lapse analysis in hippocampal slices. *Glia* **33** (3): 256–266.
3. Kaltschmidt B, Kaltschmidt C (2010) NF-kappaB in the nervous system. *Cold Spring Harb Perspect Biol*. **1** (3):a001271. doi: 20066105.
4. Sun SC (2017). The non-canonical NF-κB pathway in immunity and inflammation. *Nat. Rev. Immunol.* **17** (9), 545-558.
5. Thawkar BS, Kaur G (2019). Inhibitors of NF-κB and P2X7/NLRP3/Caspase 1 pathway in microglia: Novel therapeutic opportunities in neuroinflammation induced early-stage Alzheimer's disease. *J. Neuroimmunol*. **326**: 62-74.
6. Jie Z, Ko CJ, Wang H, Xie X, Li Y, Gu M, Zhu L, Yang JY, Gao T, Ru W, Tang SJ, Cheng X, Sun SC (2021) Microglia promote autoimmune inflammation via the noncanonical NF-κB pathway. *Sci Adv*. **7** (36): eabh0609. https://doi.org/10.1126/sciadv.abh0609
7. De Jesús TJ, Ramakrishnan P (2020). NF-κB c-Rel dictates the inflammatory threshold by acting as a transcriptional repressor. *iScience* **23** (3): 100876, https://doi.org/10.1016/j.isci.2020.100876.
8. Muxel SM, Laranjeira-Silva MF, Carvalho CE, Floeter-Winter LM, Markus RP (2016). The RelA/cRel nuclear factor-κB (NF- κB) dimer, crucial for inflammation resolution, mediates the transcription of the key enzyme in melatonin synthesis in RAW 264.7 macrophages. *J Pineal Res*. **60** (4): 394–404.
9. Carvalho-Sousa CE, Pereira EP, Kinker GS, Veras M, Ferreira ZS, Barbosa-Nunes FP, Markus RP (2020). Immune-pineal axis protects rat lungs exposed to polluted air. *J. Pineal Res.* **68** (3): 1–13.
10. Markus RP, Cecon E, Pires-Lapa MA (2013) Immune-pineal axis: Nuclear factor κB (NF-κB) mediates the shift in the melatonin source from pinealocytes to immune competent cells. *Int. J. Mol. Sci.* **14** (6): 10979–10997.
11. Pires-Lapa MA, Tamura K, Salustiano EMA, Markus RP (2013) Melatonin synthesis in human colostrum mononuclear cells enhances dectin-1-mediated phagocytosis by mononuclear cells. *J. Pineal Res*. **55** (3): 240–246.
12. GaoJ, Su G, Liu J, Zhang J, Zhou J, Liu X, Zhang Z (2020). Mechanisms of inhibition of excessive microglial activation by melatonin. *J. Mol. Neurosci.* **7** (8): 1229–1236.
13. Liu W, Yu M, Xie D, Wang L, Ye C, Zhu Q, Yang L (2020) Melatonin-stimulated MSC-derived exosomes improve diabetic wound healing through regulating macrophage M1 and M2 polarization by targeting the PTEN/AKT pathway. *Stem Cell Res. Ther*. **11** (1): 1–15.
14. Markus RP, Fernandes PA, Kinker GS, da Silveira Cruz-Machado S, Marçola M (2018) Immune-pineal axis – acute inflammatory responses coordinate melatonin synthesis by pinealocytes and phagocytes. *Bri. J. Pharmacol*. **175** (16): 3239–3250.
15. Mecha M (2011) An easy and fast way to obtain a high number of glial cells from rat cerebral tissue: A beginners approach. *Protocol Exchange* **218**: 1–18.
16. Tamashiro TT, Dalgard CL, Byrnes KR (2012) Primary microglia isolation from mixed glial cell cultures of neonatal rat brain tissue. *J. Vis. Exp.* **66**: e3814, 1–5. https://doi.org/10.3791/3814.
17. Jockers R, Delagrange P, Dubocovich ML, Zlotos DP (2016) Update on melatonin receptors:

IUPHAR Review 20. *Bri. J. Pharmacol*. **173**: 2702-2725.
18. Kobayashi K, Imagama S, Ohgomori T, Hirano K, Uchimura K, Sakamoto K, Kadomatsu K (2013) Minocycline selectively inhibits M1 polarization of microglia. *Cell Death Dis*. **4** (3): e525-9. https://doi.org/10.1038/cddis.2013.54.
19. Nikodemova M, Duncan ID, Watters JJ (2006) Minocycline exerts inhibitory effects on multiple mitogen-activated protein kinases and IκBα degradation in a stimulus-specific manner in microglia. *J. Neurochem*. **96** (2): 314–323.
20. Franco DG, Markus RP (2014) The cellular state determines the effect of melatonin on the survival of mixed cerebellar cell culture. *PLOS One* **9** (9): 25–27.
21. Kaltschmidt B, Widera D, Kaltschmidt C (2005) Signaling via NF-κB in the nervous system. *Biochim. Biophys. Acta.* **1745** (3): 287–299.
22. Muxel SM, Pires-Lapa MA, Monteiro AWA, Cecon E, Tamura EK, Floeter-Winter L M, Markus RP (2012) NF-κB drives the synthesis of melatonin in RAW 264.7 macrophages by inducing the transcription of the arylalkylamine-N-acetyltransferase (AA-NAT) gene. *PLOS ONE* **7** (12): e52010. https://doi.org/10.1371/journal.pone.0052010.
23. Bernier LP, Bohlen CJ, York EM, Choi HB, Kamyabi A, Dissing-Olesen L, MacVicar BA (2019) Nanoscale surveillance of the brain by microglia via cAMP-regulated filopodia. *Cell Rep.* **27** (10): 2895-2908.e4. https://doi.org/10.1016/j.celrep.2019.05.010.
24. Wu UI, Mai FD, Sheu JN, Chen LY, Liu YT, Huang HC, Chang HM. (2011) Melatonin inhibits microglial activation, reduces pro-inflammatory cytokine levels, and rescues hippocampal neurons of adult rats with acute Klebsiella pneumoniae meningitis. *J. Pineal Res.* **50** (2) ; 159–170.
25. Berkiks I, Benmhammed H, Mesfioui A, Ouichou A, El Hasnaoui A, Mouden S El Hessni A (2018) Postnatal melatonin treatment protects against affective disorders induced by early-life immune stimulation by reducing the microglia cell activation and oxidative stress. *Int. J. Neurosci.* **128** (6): 495–504.
26. Hu L, Zhang S, Wen H, Liu T, Cai J, Du D, Xia C (2019) Melatonin decreases M1 polarization via attenuating mitochondrial oxidative damage depending on UCP2 pathway in prorenin-treated microglia. *PLOS ONE*. **14** (2): 1–18.
27. Park E, Chun H S (2017) Melatonin attenuates manganese and lipopolysaccharide-induced inflammatory activation of BV2 microglia. *Neurochem. Res*. **42** (2): 656–666.
28. Zhang Y, Liu Z, Zhang W, Wu Q, Zhang Y, Liu, Y, Chen X (2019) Melatonin improves functional recovery in female rats after acute spinal cord injury by modulating polarization of spinal microglial/macrophages. *J. Neurosci. Res*. **97** (7): 733–743.
29. Leung JWH, Cheung TK (2021) Melatonin attenuates microglial activity and omproves neurological functions in rat model of collagense-induced intracerebral hemorrage. *Melatonin Res*. 4 (2): 360-376.
30. Pontes GN, Cardoso EC, Carneiro-Sampaio MMS, Markus RP (2006) Injury switches melatonin production source from endocrine (pineal) to paracrine (phagocytes) - Melatonin in human colostrum and colostrum phagocytes. *J. Pineal Res*. **41** (2): 136–141.
31. Pinato L, da Silveira Cruz-Machado S, Franco DG, Campos LMG, Cecon E, Fernandes PACM, Markus RP (2015) Selective protection of the cerebellum against intracerebroventricular LPS is mediated by local melatonin synthesis. *Brain Struct. Funct*. **220** (2): 827–840.
32. Ohsawa K, Imai Y, Sasaki Y, Kohsaka S (2004) Microglia/macrophage-specific protein Iba1 binds to fimbrin and enhances its actin-bundling activity. *J. Neurochem*. **88** (4): 844–856.

33. Chhor V, Le Charpentier T, Lebon S, Oré MV, Celador IL, Josserand J, Fleiss B (2013) Characterization of phenotype markers and neuronotoxic potential of polarised primary microglia *in vitro*. *Brain Behav. Immun*. **32**: 70–85.
34. Hoogland ICM, Westhoff D, Engelen-Lee JY, Melief J, Valls Serón M, Houben-Weerts JHMP, van de Beek D (2018) Microglial activation after systemic stimulation with lipopolysaccharide and *Escherichia coli*. Front. Cell. Neurosci. **12**: 110.
35. Cherry JD, Olschowka JA, Banion MK O (2014) Neuroinflammation and M2 microglia : the good , the bad , and the inflamed, *J Neuroinflammation*. **11** (1): 1–15.
36. Lee M, Rey K, Besler K, Wang C, Choy J (2017) Immunobiology of nitric oxide and regulation of inducible nitric oxide synthase. Results Probl. Cell. Differ. **6**2: 181–207.
37. Caldwell RW, Rodriguez PC, Toque HA, Narayanan SP, Caldwell RB (2018) Arginase: A multifaceted enzyme important in health and disease. *Physiol. Rev*. **98** (2): 641–665.
38. Hamzei Taj S, Kho W, Riou A, Wiedermann D, Hoehn M (2016) miRNA-124 induces neuroprotection and functional improvement after focal cerebral ischemia. *Biomaterials* **91**: 151–165.

Please cite this paper as:
Souza, E.S., Santos, A.A., Ribeiro-Paz, E.E., Córdoba-Moreno, M., Trevisan, I.L., Caldeira, W., Muxel, S.M., Sousa, K.D. and Markus, R.P. 2022. Melatonin synthesized by activated microglia orchestrates the progression of microglia from a pro-inflammatory to a recovery/repair phenotype. *Melatonin Research*. 5, 1 (Mar. 2022), 55-67. DOI:https://doi.org/https://doi.org/10.32794/mr112500120.